

Response surface methodology approach for optimization of Cu^{2+} , Ni^{2+} and Pb^{2+} adsorption using KOH-activated carbon from banana peel



Tran Van Thuan^a, Bui Thi Phuong Quynh^a, Trinh Duy Nguyen^a, Van Thi Thanh Ho^b, Long Giang Bach^{a,*}

^a NTT Institute of High Technology, Nguyen Tat Thanh University, Ho Chi Minh City, Viet Nam

^b Hochiminh City University of Natural Resources and Environment (HCMUNRE), Viet Nam

ARTICLE INFO

Article history:

Received 6 June 2016

Revised 23 October 2016

Accepted 25 October 2016

Available online 2 November 2016

Keywords:

Adsorption of heavy metal ions

Banana peel

Response surface methodology

Activated carbon

ABSTRACT

This study aims at optimizing the adsorption of heavy metal ions onto banana peel derived activated carbon (AC) using response surface methodology (RSM) involving central composite design (CCD). The cheap, non-toxic and locally available banana peel was subjected to carbonization and subsequently KOH-activation to produce the porous AC, which was then characterized by SEM and FTIR analyses. In RSM study, the individual and interactive effects of three critical variables including heavy metal ion concentration, pH of solution and AC dosage on the adsorption capacity were optimized. The maximum adsorption capacity appeared to follow the order: Cu^{2+} (14.3 mg/g) < Ni^{2+} (27.4 mg/g) < Pb^{2+} (34.5 mg/g) that agreed well with the verification experiments, revealing the reliability and suitability of the optimization approach. In addition, the results of isotherm study show that the Langmuir model can be used to best describe the adsorption behavior of Cu^{2+} and Ni^{2+} onto the banana peel derived activated carbon.

© 2016 Elsevier B.V. All rights reserved.

1. Introduction

In recent years, removal of pollutants using activated carbons (ACs) fabricated from low-cost natural resources has been realized as a green and cost-efficient solution to the currently challenging environmental problems [1–3]. Many studies have demonstrated the possibility of converting a variety of non-toxic, cheap and abundant agricultural wastes, such as coconut shell, tea waste, rice husk, sugar cane bagasse, fruit peels, into low-cost but high-performance ACs [4–8]. Some agriculture waste derived activated carbons with outstanding properties like large surface area, diverse functional groups, and high porosity were reported to exhibit high efficiency in adsorption of various organic and inorganic toxicants [9,10]. Hence, they are concerned as appropriate alternatives to costly commercial activated carbons which are often produced from non-renewable and expensive precursors.

Hazardous metal contamination in water has long existed as a serious threat to human health and aquatic life due to the persistence of the heavy metals in nature. The discharge of heavy metals into water sources is often resulted from leaks of chemical pollutants, mineral processing and many other kinds of manufacturing activities. Although trace amounts of some transition met-

als, e.g. copper, nickel and lead, are essential for living organisms, their excessive levels may cause very harmful effects like neurological disorders, respiratory failure, birth defects or even death in extreme poison [11]. The major obstacle to decontamination of heavy metals is either the high-cost or low-efficiency of conventional treatment methods, including oxidation/reduction, coagulation and flocculation, reverse osmosis, membrane filtration, ion exchange and electrochemical techniques [12,13]. However, adsorption process using activated carbon adsorbent is especially favored due to its high efficiency, easy operation, insensitivity to toxic substances, the possibility of reuse and large scale promotion [14]. The efficiency of adsorption process crucially depends on the property of adsorbents and selection of suitable operation conditions. The first factor is normally controlled by the nature of source materials and fabrication strategy while the latter requires an appropriate combination of different influential factors which often needs to be determined via a large number of tests. However, by applying optimization tools, a number of experiments can be significantly reduced. Response surface methodology (RSM) involving a group of mathematical and statistical techniques that are based on the fit of empirical models to the experimental data obtained from a set of designed experiments is considered as one of the most relevant multivariate techniques used in analytical optimization [15]. Among several matrix designs with different properties and characteristics, CCD is more commonly applied to define which experiments should be carried out in the examined experimental region

* Corresponding author. Fax: +84 83940 4759.
E-mail address: blgiangntt@gmail.com (L.G. Bach).

to evaluate individual and interaction effects of independent variables with least number of experiments [16].

Banana is a kind of tropical fruit massively cultivated and consumed in hundreds of countries. Recently, cheap and abundant banana tree originated agricultural wastes have also attracted much attention for their potential applications in remediation of waste water contaminated by heavy metals, dyes and various organic pollutants [8,17–19]. However, as far as we are concerned, few research has focused on the fabrication and exploration of adsorption characteristics of the banana peel derived activated carbon. Therefore, this study aims at employing the RSM involving CCD to study the individual and interactive effects of influential factors on the adsorption of heavy metals using the banana peel derived activated carbon, thereby defining the optimum region for maximum adsorption capacity. In the fabrication process, chemical activation using KOH was applied to form porous carbon structure as it has been well-known to be efficient and eco-friendly [20–22]. The adsorption tests were performed with three common heavy metals including Cu^{2+} , Ni^{2+} , Pb^{2+} ions. The quadratic polynomial regression model involving three independent variables, i.e. concentration of heavy metal ions, adsorbent dosage, pH and taking adsorption capacity of the synthesized-AC as the main response were successfully developed. The goodness of fit of the model and the significance of influential variables were evaluated via the analysis of variance (ANOVA).

2. Experimental procedure

2.1. Fabrication of activated carbon from banana peel

The banana peels were collected from the local markets, washed with distilled water for several times, dried under the sunshine and ground into small pieces with less than 1.0 mm in diameter. The precursor was then carbonized under a nitrogen atmosphere at 500 °C for 1 h with a heating rate of 10 °C/min. The resulting char was soaked with potassium hydroxide solution for 24 h. The ratio between the char and KOH was 1:1 (wt%). The KOH-impregnated char was further heated under nitrogen at 500 °C for 0.5 h. Finally, the as-received KOH-activated carbon was repeatedly washed with deionized water until approaching neutral pH followed by drying at 105 °C for 24 h.

2.2. Instruments and techniques

The X-ray powder diffraction (XRD) of AC was implemented on D8 Advance Bruker powder diffractometer with a $\text{Cu-K}\alpha$ excitation source. The diffraction spectra were recorded with a scan rate of 0.02°/s. The angle range (2θ) was investigated between 0° and 50°. The morphological study of the material surface was identified by scanning electron microscope (SEM) technique on an S4800 instrument, Japan at an accelerating voltage source of 10 kV. The FT-IR spectra were recorded using the Nicolet 6700 spectrophotometer instrument.

2.3. Batch adsorption experiments

The adsorption experiments were carried out in the Erlenmeyer flasks containing 50 mL of aqueous solution of M (II) ions ($\text{M} = \text{Cu}$, Pb , and Ni) and the synthesized activated carbon. Input factors were investigated including initial M (II) concentration (8.0–92.0 ppm), adsorbent dosage (0.8–9.2 g/L) and pH of the solution (0.6–7.4). The mixture was mixed thoroughly until obtaining the adsorption equilibrium. The residual concentrations of heavy metals were confirmed by AAS analysis. The removal efficiency and

Table 1
Independent variables matrix and their encoded levels.

| No | Independent factors | Code | Levels | | | | |
|----|----------------------------|-------|-----------|------|-----|------|-----------|
| | | | $-\alpha$ | -1 | 0 | $+1$ | $+\alpha$ |
| 1 | M (II) concentration (ppm) | x_1 | 8.0 | 25 | 50 | 75 | 92.0 |
| 2 | Dosage of AC (g/L) | x_2 | 0.8 | 2.5 | 5 | 7.5 | 9.2 |
| 3 | pH of solution (–) | x_3 | 0.6 | 2 | 4 | 6 | 7.4 |

the adsorption capacity were calculated as follows:

$$M \text{ (II) removal (\%)} = \frac{C_o - C_f}{C_o} \cdot 100 \quad (1)$$

where C_o and C_f are the initial and equilibrium M (II) concentrations (ppm) respectively.

$$q_f \text{ (mg/g)} = \frac{C_o - C_f}{W} \cdot V = \frac{C_o - C_f}{d_{AC}} \quad (2)$$

Where V (mL) is the volume of the M (II) solution, W (g) is the weight of the adsorbent, d_{AC} (g/L) is the dosage of the AC.

2.4. Experimental design with RSM

Response surface methodology, which combines the advantages of mathematical and statistical techniques, is widely applied as a powerful tool to obtain responses over the entire factor space and determine the region of optimal or near-optimal response using a sequence of designed experiments. The concept of a typical response surface method involves an independent variable “ y ” called the response variable and several independent variables x_i ($i = 1, 2, 3, 4, \dots, k$). Second order polynomial model is usually utilized to establish the functional relationship between y and the set of independent values “ x_i ”. Generally, the main steps of RSM are as follows: (1) the selection of independent variables representing major effects on the system; (2) the choice of the experimental design and accordingly conducting the experiments; (3) the mathematical-statistical treatment of the obtained experimental data through the fit of a polynomial function; (4) the evaluation of the model's fitness, and (5) the determination of the optimum values [23,24]. In the present study, RSM superimposed with central composite design (CCD) was employed to study the significance of independent variables and thereby determining optimal conditions for adsorption process. In details, metal ions (Cu^{2+} , Pb^{2+} , Ni^{2+}) concentration (x_1), the dosage of adsorbent (x_2), and pH (x_3) were taken as three input variables and the adsorption capacity (y) of the activated carbon towards metal ions was taken as the response (Table 1). The CCD for three independent variables was designed based on 4 axial points, 8 factorial points, and 6 replicates at the center points; the total number of experiment is calculated using the following equation:

$$N = 2^k + 2k + c = 2^3 + 2 \cdot 3 + 6 = 20 \quad (3)$$

where k is the number of factors, c is the number of center points.

The adsorption capacity is correlated to the independent variables using the following second order polynomial model that takes into account the individual, interactive and quadratic terms as follows [25]:

$$y = \beta_o + \sum_{i=1}^k \beta_i x_i + \sum_{i=1}^k \sum_{j=1}^k \beta_{ij} x_i x_j + \sum_{i=1}^k \beta_{ii} x_i^2 \quad (4)$$

where y is the predicted response; x_i and x_j are the independent variables. The parameter β_o , β_i , β_{ij} , and β_{ii} , are the regression coefficients for intercept, linear effect, double interaction, and quadratic effect, respectively.

Analysis of variance (ANOVA) of the quadratic polynomial regression models was utilized to identify the significance of input

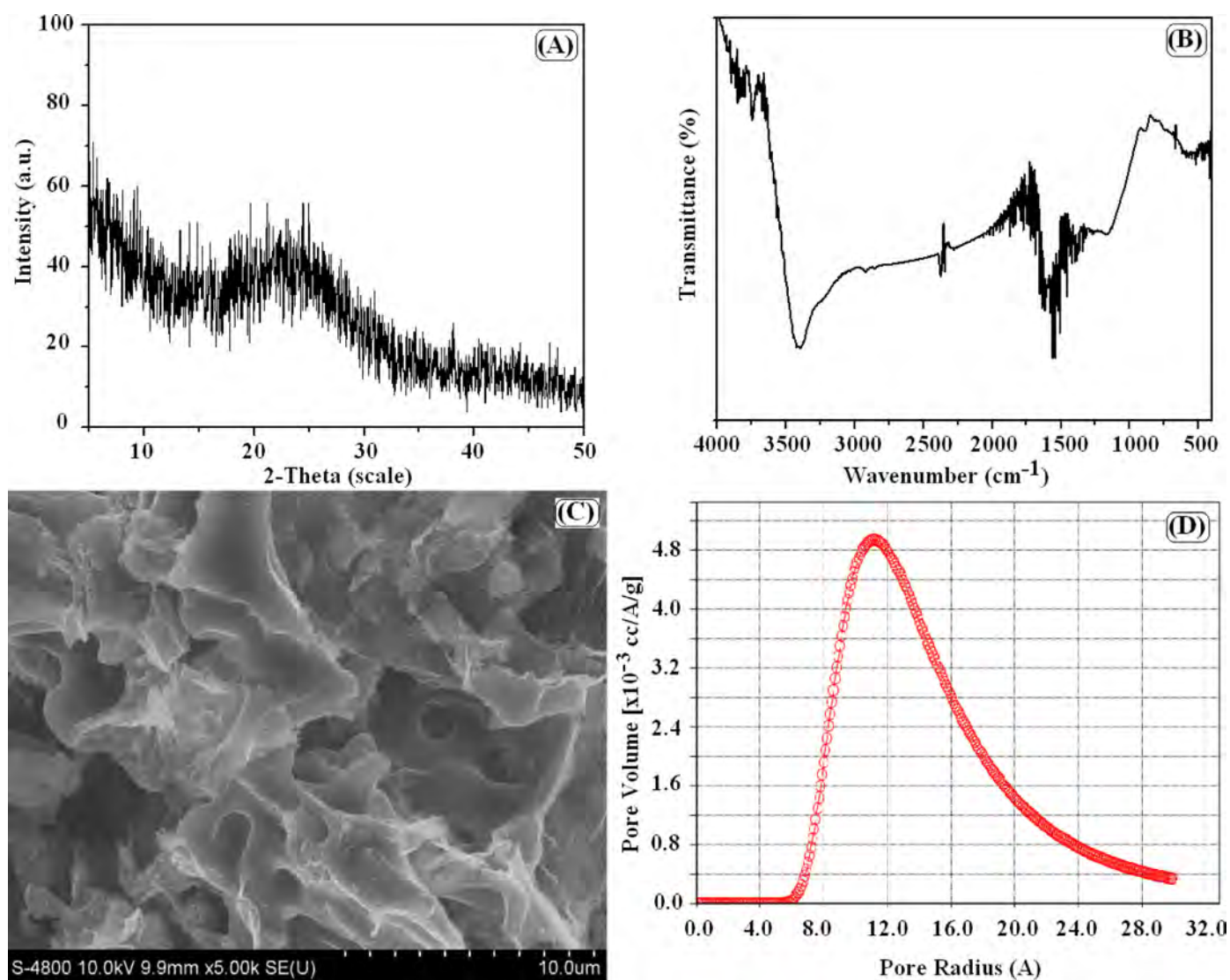


Fig. 1. (A) XRD spectra, (B) FT-IR spectra, (C) SEM micrograph and (D) pore size distribution of the AC.

variables as well as the relationship between the responses and the influential factors [26]. In this study, the ANOVA was calculated using Design-Expert version 9.0.5.1 (DX9).

3. Results and discussion

3.1. Characterization of the banana peel derived activated carbon (AC)

The structure of banana peel based AC was first characterized using XRD analysis as presented in Fig. 1A. The presence of a broad peak in the range of 20° – 30° demonstrates the typical amorphous structure of amorphous carbon [27–29]. Moreover, the absence of sharp peaks indicates the negligible existence of residual ash in the structure.

The as-synthesized AC was found to possess a complex surface structure containing various kinds of functional groups according to the FT-IR analysis (Fig. 1B). The broad adsorption band from ca. 3330 cm^{-1} to ca. 3450 cm^{-1} is attributable the stretching vibrations of free and intermolecular bonded O–H groups. The presence of the C=O group and O–N asymmetric stretch can be verified by the adsorption bands at 1700 cm^{-1} and 1541 cm^{-1} , respectively. A minor peak at 2916 cm^{-1} identified the presence

of stretching vibration of the C–H group. Moreover, the peak at 1640 cm^{-1} may correspond to the C=C stretching or to the asymmetric and symmetric stretching vibrations of C–O while that detected at 2353 cm^{-1} could be ascribed to the C≡C [30–32].

The synthesized banana peel derived AC has a highly porous, rich-defect structure as revealed by SEM analysis (Fig. 1C). The measurement of N_2 adsorption/desorption isotherm at -196°C provided the BET surface area of $63.5\text{ m}^2/\text{g}$. According to the pore distribution determined via DA method (Fig. 1D), the radii of micropores and mesopores in the AC ranged from around 5 \AA to 20 \AA with the average pore radius at 11.1 \AA and micropore volume of $0.014\text{ cm}^3/\text{g}$. As expected, the formation of pore system of the AC resulted from the rapid emission of species during carbonization process and from the development of new micropores induced by KOH activation. It was suggested that KOH could promote both the generation of new micropores and the enlargement of as-existing micropores to mesopores [33].

3.2. Quadratic models for adsorption of heavy metal ions onto the banana peel derived activated carbon (AC)

CCD design matrix was established to investigate the contribution of three influential factors including metal ion concentration,

Table 2.
Matrix of observed and predicted values.

| Run | Independent factors | | | Experiment of removal (%) | | | Experiment of uptake (mg/g) | | | Prediction of uptake (mg/g) | | |
|-----|---------------------|-------|-------|---------------------------|------------------|------------------|-----------------------------|---------------|---------------|-----------------------------|---------------|---------------|
| | x_1 | x_2 | x_3 | Cu ²⁺ | Ni ²⁺ | Pb ²⁺ | $q_{Cu^{2+}}$ | $q_{Ni^{2+}}$ | $q_{Pb^{2+}}$ | $q_{Cu^{2+}}$ | $q_{Ni^{2+}}$ | $q_{Pb^{2+}}$ |
| 1 | 25 | 2.5 | 2 | 19.0 | 3.6 | 41.2 | 1.90 | 0.36 | 4.12 | 1.74 | 0.64 | 2.11 |
| 2 | 75 | 2.5 | 2 | 7.7 | 31.7 | 55.3 | 2.32 | 9.52 | 16.60 | 2.96 | 9.07 | 13.73 |
| 3 | 25 | 7.5 | 2 | 8.1 | 27.9 | 88.5 | 0.27 | 0.93 | 2.95 | 0.23 | 1.38 | 1.89 |
| 4 | 75 | 7.5 | 2 | 11.6 | 74.3 | 27.7 | 1.16 | 7.43 | 2.77 | 1.94 | 7.44 | 1.77 |
| 5 | 25 | 2.5 | 6 | 71.7 | 96.4 | 94.2 | 7.17 | 9.64 | 9.42 | 7.89 | 10.62 | 9.56 |
| 6 | 75 | 2.5 | 6 | 47.3 | 71.0 | 92.7 | 14.2 | 21.3 | 27.80 | 11.55 | 21.85 | 29.13 |
| 7 | 25 | 7.5 | 6 | 98.1 | 98.7 | 99.9 | 3.27 | 3.29 | 3.33 | 3.53 | 1.75 | 2.16 |
| 8 | 75 | 7.5 | 6 | 72.4 | 98.9 | 100 | 7.24 | 9.89 | 10.00 | 7.68 | 10.61 | 9.98 |
| 9 | 8 | 5 | 4 | 98.1 | 96.9 | 100 | 1.57 | 1.55 | 1.60 | 0.99 | 1.93 | 1.12 |
| 10 | 92 | 5 | 4 | 64.1 | 99.2 | 99.7 | 11.8 | 18.26 | 18.35 | 5.50 | 16.46 | 17.47 |
| 11 | 50 | 0.8 | 4 | 13.6 | 21.8 | 36.0 | 8.5 | 13.60 | 22.50 | 9.62 | 14.89 | 21.43 |
| 12 | 50 | 9.2 | 4 | 98.3 | 98.8 | 99.9 | 5.34 | 5.37 | 5.43 | 5.10 | 6.06 | 5.14 |
| 13 | 50 | 5 | 0.6 | 1.8 | 0.2 | 2.6 | 0.18 | 0.02 | 0.26 | -1.02 | -1.10 | -2.59 |
| 14 | 50 | 5 | 7.4 | 98.8 | 98.9 | 90.9 | 9.88 | 9.89 | 9.09 | 8.97 | 9.95 | 10.58 |
| 15 | 50 | 5 | 4 | 75.4 | 97.7 | 99.2 | 7.54 | 9.77 | 9.92 | 7.64 | 9.87 | 9.96 |
| 16 | 50 | 5 | 4 | 77.4 | 93.1 | 100 | 7.74 | 9.31 | 10.00 | 7.64 | 9.87 | 9.96 |
| 17 | 50 | 5 | 4 | 73.8 | 93.8 | 95.1 | 7.38 | 9.38 | 9.51 | 7.64 | 9.87 | 9.96 |
| 18 | 50 | 5 | 4 | 75.6 | 97.9 | 96.5 | 7.56 | 9.79 | 9.65 | 7.64 | 9.87 | 9.96 |
| 19 | 50 | 5 | 4 | 80.3 | 94.2 | 100 | 8.03 | 9.42 | 10.00 | 7.64 | 9.87 | 9.96 |
| 20 | 50 | 5 | 4 | 72.2 | 97.3 | 95.8 | 7.22 | 9.73 | 9.58 | 7.64 | 9.87 | 9.96 |

x_1 : Initial concentration, x_2 : adsorbent dosage, x_3 : pH of solution.

pH and dosage of banana peel based activation carbon the adsorption of Pb²⁺, Cu²⁺, and Ni²⁺. Five levels of the variables including the low (encoded -1), high (encoded +1) and rotatable (encoded $\pm\alpha$) one were defined. The adsorption capacity, taken as the main response, was predicted using polynomial regression equation in which the main, interaction and quadratic effects of the variables were modeled.

Table 2 exhibits the experimental design of 20 runs along with the experimental and predicted adsorption results for Pb²⁺, Cu²⁺, and Ni²⁺. It can be observed that the adsorption capacities vary strongly depending on the values of the influential factors. However, the results at center points demonstrated nearly 100% removal of Pb²⁺ and Ni²⁺ while the elimination of Cu²⁺ was lower at around 70–80%. The main contents of Table 3 include the results of the analysis of variance (ANOVA) fitted to the second-order polynomial equations and the corresponding regression coefficients. Statistical significance and accuracy of the models can be confirmed via high *F*, low *p*-value, correlation coefficient (*R*) close to 1, and the results of lack of fit (LOF) test. A *p*-value less than 0.05 demonstrates the statistical significance of factor effect (at 95% confidence level). The LOF value parameter showed the variation of response around the fitted model; this parameter appears insignificant if the model fits data well. According to these standards, the high *F*-values of all three models with Prob. > *F* values lower than 0.0001 as presented in Table 3 suggest the statistical significance of the models. Note that the proposed models fitted to the real responses for Ni²⁺ and Pb²⁺ better than that for Cu²⁺. The values of *R*² and adjusted *R*² are higher than 0.99 for Ni²⁺, Pb²⁺ while those for Cu²⁺ were lower, at 0.9394 and 0.8849 respectively. Moreover, the lack of fit tests suggests the statistical significance of the models for Ni²⁺ and Pb²⁺. In the case of Cu²⁺, the significance of LOF may occur due to the involvement of other influential factors.

The regression analysis of CCD afforded the following second order polynomial equations for Cu²⁺, Ni²⁺, and Pb²⁺ respectively:

$$q_{Cu^{2+}} = 7.61 + 2.38x_1 - 1.17x_2 + 3.34x_3 + 0.05x_1x_2 + 1.59x_1x_3 - 0.63x_2x_3 - 0.54x_1^2 - 0.46x_2^2 - 1.12x_3^2 \quad (5)$$

$$q_{Ni^{2+}} = 9.56 + 4.30x_1 - 2.42x_2 + 3.11x_3 - 0.97x_1x_2 + 0.33x_1x_3 - 2.03x_2x_3 - 0.21x_1^2 - 0.003x_2^2 - 1.61x_3^2 \quad (6)$$

$$q_{Pb^{2+}} = 9.77 + 4.80x_1 - 4.95x_2 + 2.85x_3 - 3.05x_1x_2 + 1.59x_1x_3 - 1.11x_2x_3 + 0.09x_1^2 + 1.51x_2^2 - 1.78x_3^2 \quad (7)$$

The statistical significance of each variable and the possible interactions can be seen at different degrees of probability in Table 3. The initial ion concentration, pH, and activated carbon dosage affect significantly on the adsorption capacities of all three metals. It is worth noting that all these factors also showed significant quadratic effects on the adsorption of Pb²⁺ and Ni²⁺.

Fig. 2 shows the graphs of actual versus predicted data obtained from the adsorption of three metals. The graph of Cu²⁺ as displayed in Fig. 2A show some deviations between the expected and observed values. However, they were still closely distributed to the line indicating a relative compatibility. On the other hand, the plots for Ni²⁺ and Pb²⁺ (Fig. 2B and C) reveal the well-fitting with high correlation coefficients suggesting a high adequacy of the models. The above evaluations demonstrate that the derived quadratic equations are suitable to predict the adsorption of such ion metals under the examined conditions involving the effects of metal ion concentration, the dosage of banana raw based activated carbon and pH value.

3.3. Effect of influential factors on the adsorption of heavy metal ions onto the banana peel derived activated carbon (AC)

Three-dimensional curves were plotted to clarify the effects of process variables, with two factors for each graph, on the predicted metal uptake and to locate the optimal or near-optimal adsorption regions. The combined effect of ion concentration (8–92 ppm), and AC dosage (0.8–9.2 g/L) on the Cu²⁺, Ni²⁺, and Pb²⁺ uptake at pH = 4 is exhibited in Fig. 3. For all three metals, it is generally found in all three metals that the adsorption efficiency appears inappreciable in the low concentration range (<25 ppm) but the higher initial concentration affords more considerable uptake capacity at all levels of AC dosages. This is well consistent with the assumption that active sites of the AC can capture more metal ions when their densities in the solution get higher thus leading to increase in adsorption capacities [34,35]. According to Fig. 3A, the adsorption capacity for Cu²⁺ generally decreases with increasing adsorbent dosage at various concentrations and the metal uptake went up as the concentration rises from 8 ppm to around 66 ppm before dropping down at all dosages of AC. In terms of Ni²⁺ and Pb²⁺, the effect of AC dosage increases as the concen-

Table 3
ANOVA for absorption of Cu²⁺, Ni²⁺ and Pb²⁺.

| Response | Source | Sum of squares | Degree of freedom | Mean square | F-value | Prob > F | Comment |
|--------------------------------|--------------------------------|----------------|-------------------|-------------|---------|----------------------|---|
| Cu ²⁺ uptake (mg/g) | Model | 293.64 | 9 | 32.63 | 30.42 | <0.0001 ^s | SD = 1.04 |
| | x ₁ | 77.41 | 1 | 77.41 | 72.17 | <0.0001 ^s | Mean = 6.16 |
| | x ₂ | 18.66 | 1 | 18.66 | 17.40 | 0.0019 ^s | CV = 16.8 |
| | x ₃ | 151.92 | 1 | 151.92 | 141.65 | <0.0001 ⁿ | Press = 78.89 |
| | x ₁ ² | 0.021 | 1 | 0.021 | 0.020 | 0.8915 ^s | R ² = 0.9648 |
| | x ₂ ² | 20.13 | 1 | 20.13 | 18.77 | 0.0015 ⁿ | R ² _(adj.) = 0.9330 |
| | x ₃ ² | 3.21 | 1 | 3.21 | 3.00 | 0.1142 ⁿ | AP = 21.469 |
| | x ₁ x ₂ | 4.21 | 1 | 4.21 | 3.92 | 0.0759 ^s | |
| | x ₁ x ₃ | 3.01 | 1 | 3.01 | 2.81 | 0.1248 ⁿ | |
| | x ₂ x ₃ | 18.23 | 1 | 18.23 | 16.99 | 0.0021 ⁿ | |
| | Residuals | 10.73 | 10 | 1.07 | – | – | |
| | Lack of fit | 10.33 | 5 | 2.07 | 25.84 | 0.0014 ⁿ | |
| | Pure error | 0.40 | 5 | 0.080 | – | – | |
| | Ni ²⁺ uptake (mg/g) | Model | 543.16 | 9 | 60.35 | 438.10 | <0.0001 ^s |
| x ₁ | | 251.95 | 1 | 251.95 | 1828.98 | <0.0001 ^s | Mean = 8.32 |
| x ₂ | | 80.33 | 1 | 80.33 | 583.11 | <0.0001 ^s | CV = 4.46 |
| x ₃ | | 132.03 | 1 | 132.03 | 958.40 | <0.0001 ⁿ | Press = 10.12 |
| x ₁ ² | | 7.45 | 1 | 7.45 | 54.08 | <0.0001 ^s | R ² = 0.9975 |
| x ₂ ² | | 0.85 | 1 | 0.85 | 6.13 | 0.0327 ⁿ | R ² _(adj.) = 0.9952 |
| x ₃ ² | | 32.97 | 1 | 32.97 | 239.31 | <0.0001 ⁿ | AP = 80.416 |
| x ₁ x ₂ | | 0.62 | 1 | 0.62 | 4.52 | 0.0594 ^s | |
| x ₁ x ₃ | | 0.00012 | 1 | 0.00012 | 0.0008 | 0.9774 ⁿ | |
| x ₂ x ₃ | | 37.18 | 1 | 37.18 | 269.89 | <0.0001 ⁿ | |
| Residuals | | 1.38 | 10 | 0.14 | – | – | |
| Lack of fit | | 1.14 | 5 | 0.23 | 4.74 | 0.0565 ⁿ | |
| Pure error | | 0.24 | 5 | 0.048 | – | – | |
| Pb ²⁺ uptake (mg/g) | | Model | 951.54 | 9 | 105.73 | 775.64 | <0.0001 ^s |
| | x ₁ | 314.34 | 1 | 314.34 | 2306.09 | <0.0001 ^s | Mean = 9.64 |
| | x ₂ | 334.60 | 1 | 334.60 | 2454.70 | <0.0001 ^s | CV = 3.83 |
| | x ₃ | 111.15 | 1 | 111.15 | 815.40 | <0.0001 ⁿ | Press = 9.02 |
| | x ₁ ² | 74.24 | 1 | 74.24 | 544.63 | <0.0001 ^s | R ² = 0.9986 |
| | x ₂ ² | 20.32 | 1 | 20.32 | 149.08 | <0.0001 ⁿ | R ² _(adj.) = 0.9973 |
| | x ₃ ² | 9.88 | 1 | 9.88 | 72.48 | <0.0001 ⁿ | AP = 107.26 |
| | x ₁ x ₂ | 0.12 | 1 | 0.12 | 0.88 | 0.3705 ^s | |
| | x ₁ x ₃ | 32.51 | 1 | 32.51 | 238.48 | <0.0001 ⁿ | |
| | x ₂ x ₃ | 45.80 | 1 | 45.80 | 335.98 | <0.0001 ⁿ | |
| | Residuals | 1.36 | 10 | 0.14 | – | – | |
| | Lack of fit | 1.12 | 5 | 0.22 | 4.54 | 0.0612 ⁿ | |
| | Pure error | 0.25 | 5 | 0.049 | – | – | |

Note: ^s significant at $p < 0.05$, ⁿ insignificant at $p > 0.05$.

tration increases; the higher concentration and lower AC dosage lead to higher metal uptake over the examined ranges (Fig. 3B and C). The correlation of pH (0.6–7.4) and metal ion concentration (8–92 ppm) is presented in Fig. 4. The adsorption of Cu²⁺ hardly occurs in strongly acidic solution (pH < 2) regardless of initial concentration. A similar picture is observed for Ni²⁺ and Pb²⁺ in low concentration range but the concentration higher than 75 ppm can afford considerable adsorption. The adsorption appears to be more favored as pH approaches neutral value (5.7–7.4). This can be explained that higher pH value supports higher concentration and high mobility of the H⁺ that is preferably adsorbed onto the AC thus resulting in less adsorption of heavy metal ions.

Fig. 5 illustrates the remarkable relation between AC dosage and pH value with relatively similar trends observed for all three metals. In strongly acidic solution (pH < 2) the metal uptake is almost undetected regardless of the AC amount added. The increase of adsorption capacity due to the increase of pH value (pH > 2) is more significant as the AC dosage decreases. In other words, the change of pH affects more significantly with low AC dosage. According to the above results, the operation conditions to obtain maximum adsorption capacities were predicted and presented in Table 4. The maximum adsorption capacities for Cu²⁺, Ni²⁺, and Pb²⁺ are predicted to be obtained at (14.3 mg/g) < Ni²⁺ (27.4 mg/g) < Pb²⁺ (34.5 mg/g) using the initial concentration of 85 ppm, 90.3 ppm, 74.4 ppm, AC dosage of 2.4 g/L, 1.8 g/L, 0.9 g/L and pH values of 6.5, 6.4, 6.1, respectively. In experiments for model confirmation, the real adsorption capacities at the RSM derived optimum con-

ditions were obtained at 14.3 mg/g, 27.4 mg/g and 34.5 mg/g for Cu²⁺, Ni²⁺, Pb²⁺ respectively which are close to the predicted values, indicating the suitability and accuracy of the suggested models. In good agreement with other studies, the adsorption capacity for Pb²⁺ on activated carbon is stronger as compared to those for Ni²⁺ and Cu²⁺ [36–38].

3.4. Adsorption isotherm study

The adsorption isotherm models were also employed to explore the adsorption behaviors of the heavy metals onto the banana peel-derived activated carbon. Among a number of isotherm models, Langmuir and Freundlich's isotherms are most commonly used ones for describing the adsorption of heavy metals and organic compounds on ACs [34]. The Langmuir model is based on the assumption that monolayer adsorption occurs on a homogeneous surface with a finite number of adsorption sites and negligible mutual interactions between the adsorbed molecules [39,40]. The linear form of Langmuir equation is given as:

$$\frac{1}{q_e} = \frac{1}{q_m K_L C_e} + \frac{1}{q_m}$$

where C_e (mg/L) and q_e (mg/g) are equilibrium concentration and adsorption capacity, respectively. q_m (mg/g) and K_L (L/mg) are the maximum adsorption capacity and rate of adsorption (Langmuir constant), respectively.

Table 4
Model confirmation.

| Sample | Concentration (ppm) | Dosage (g/L) | pH | Capacity (mg/g) | | Removal (%) | |
|--------|---------------------|--------------|-----|-----------------|--------|-------------|--------|
| | | | | Predicted | Tested | Predicted | Tested |
| AC-Cu | 85.0 | 2.4 | 6.5 | 16.4 | 14.3 | 46.3 | 40.4 |
| AC-Ni | 90.3 | 1.8 | 6.4 | 26.2 | 27.4 | 52.2 | 54.6 |
| AC-Pb | 74.4 | 0.9 | 6.1 | 36.2 | 34.5 | 43.8 | 41.7 |

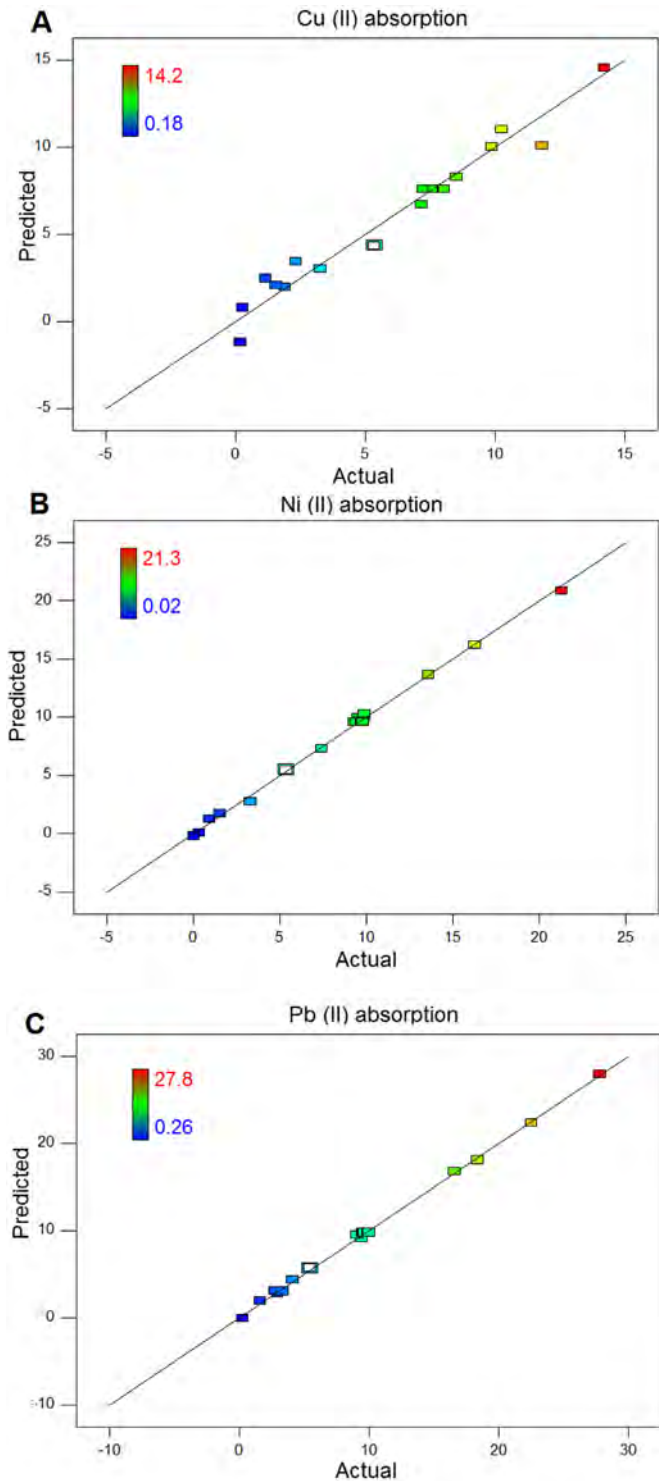


Fig. 2. Actual versus predicted data of Cu^{2+} , Ni^{2+} and Pb^{2+} adsorption.

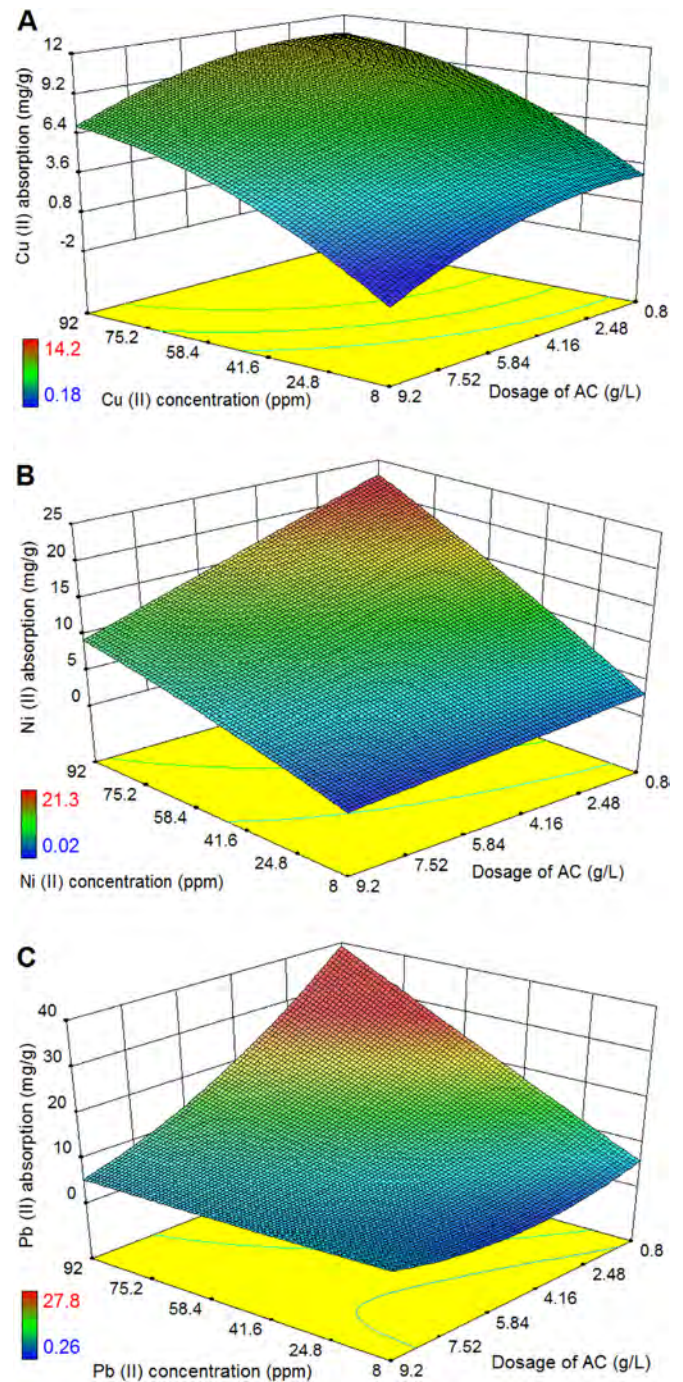


Fig. 3. Effect of initial concentration and dosage on Cu^{2+} , Ni^{2+} , Pb^{2+} uptake.

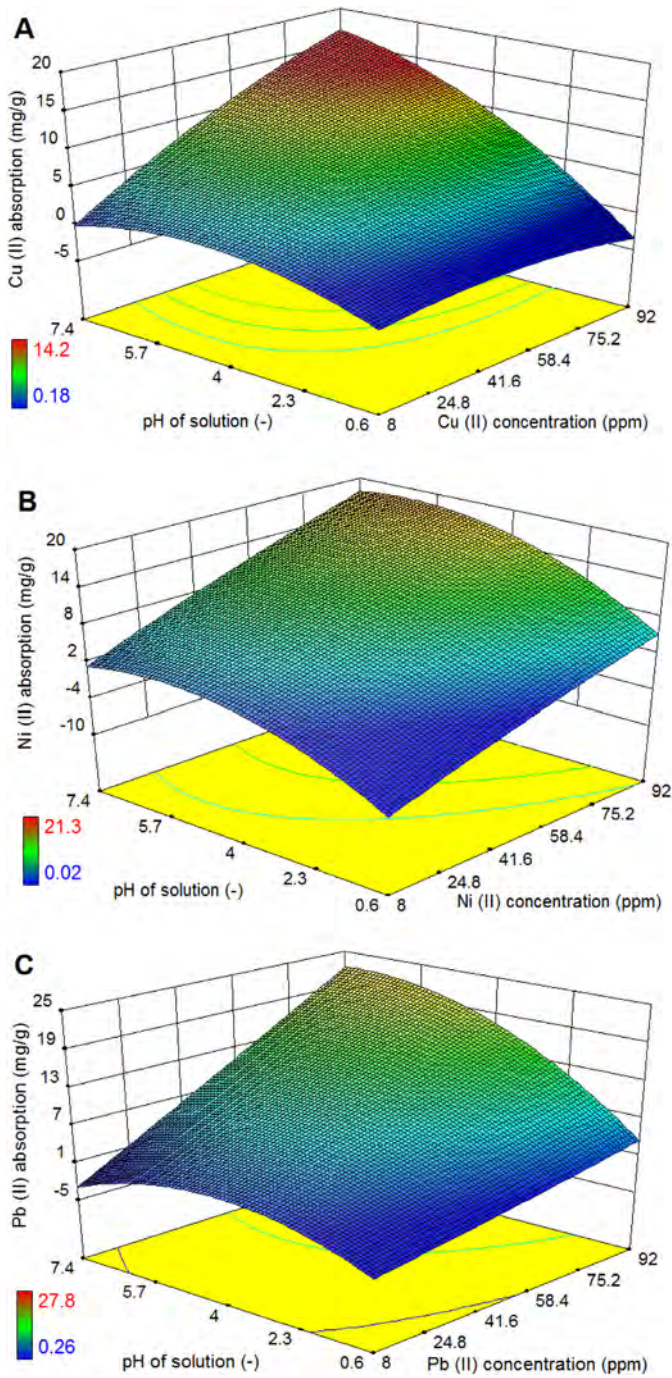


Fig. 4. Effect of pH solution and initial concentration on Cu²⁺, Ni²⁺, Pb²⁺ uptake.

Term of dimensionless equilibrium parameter (R_L) is one of the essential characteristics of the Langmuir isotherm modeling, which is defined as the following equation:

$$R_L = \frac{1}{1 + K_L C_0}$$

where K_L (L/mg) is the Langmuir constant and C_0 (mg/L) is the highest metal ion concentration. The type of the adsorption isotherm is determined by the value range of R_L : unfavorable ($R_L > 1$), linear ($R_L = 1$), favorable ($0 < R_L < 1$) and irreversible ($R_L = 0$) [40].

On the other hand, the Freundlich model assumes that molecules are adsorbed on the heterogeneous surfaces of adsorbate based on different sites with different adsorption energies

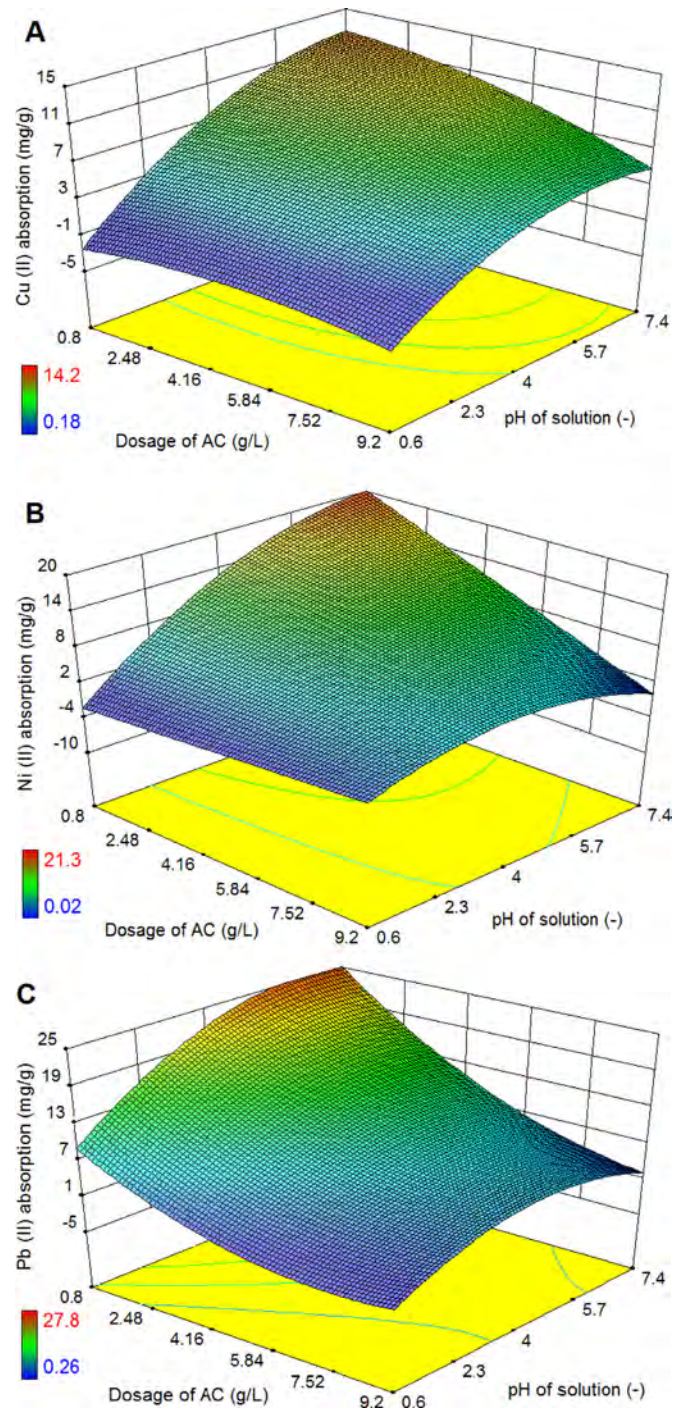


Fig. 5. Effect of dosage and pH solution on Cu²⁺, Ni²⁺, Pb²⁺ uptake.

[41,42]. This model takes into account the mutual interaction between adsorbed molecules. The application of the Freundlich equation also suggests that sorption energy exponentially decreases upon the completion of the sorption centers of the adsorbent. The linear form of Freundlich equation is given as:

$$\ln q_e = \ln K_F + \frac{1}{n} \ln C_e$$

where $1/n$ and K_F [(mg/g) · (L/mg)^{1/n}] are Freundlich constants related to the favorability of adsorption process and the adsorption capacity of the adsorbate, respectively. $1/n$ is the heterogeneity factor indicating the adsorption intensity of the adsorbent [43].

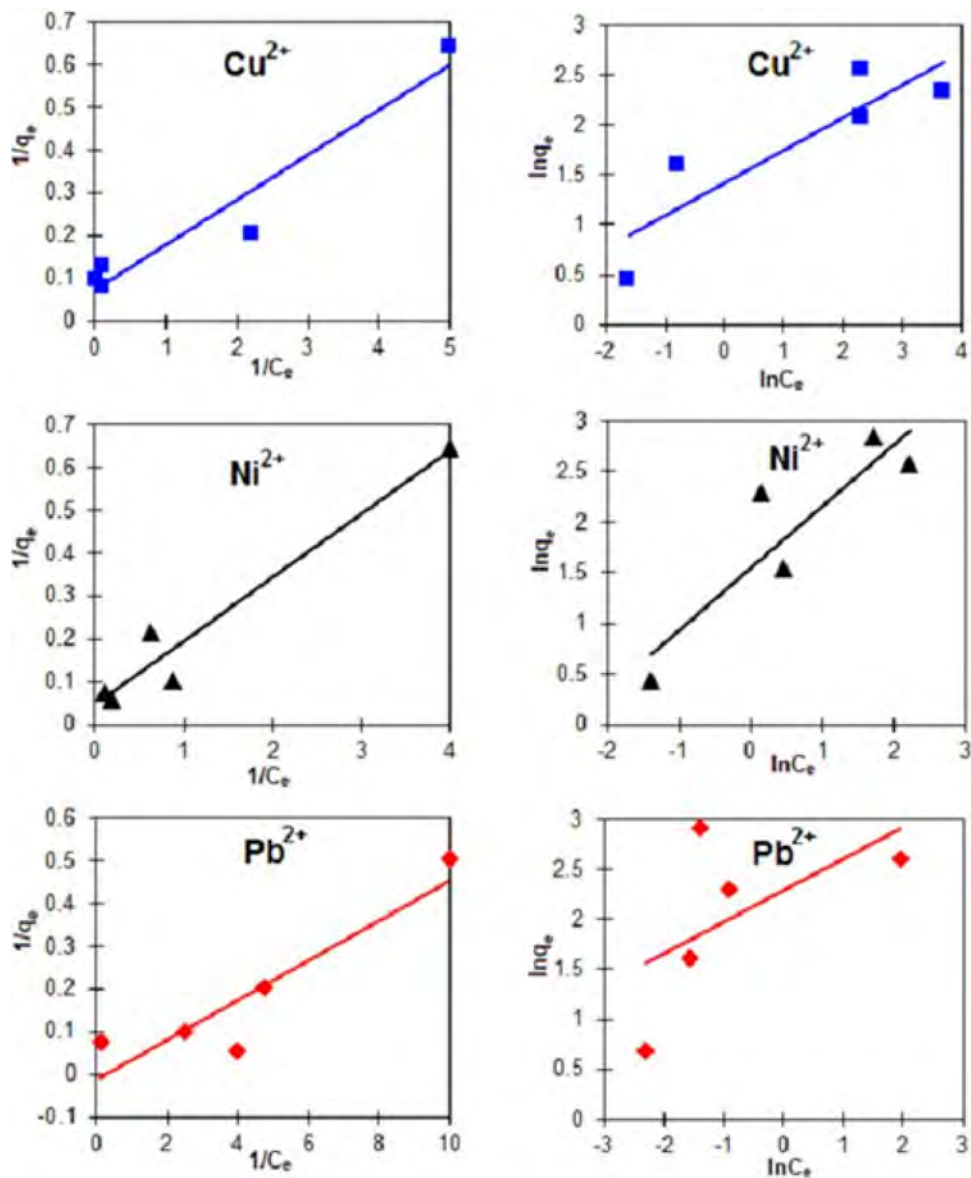


Fig. 6. Langmuir and Freundlich isotherm plots for adsorption of Cu^{2+} , Ni^{2+} and Pb^{2+} onto the AC.

Table 5
Langmuir and Freundlich isotherm constants for Cu^{2+} , Ni^{2+} , Pb^{2+} .

| Ions | Langmuir isotherm coefficient | | | | Freundlich isotherm coefficient | | |
|------------------|-------------------------------|--------------|--------|--------|--------------------------------------|--------|--------|
| | q_m (mg/g) | K_L (L/mg) | R^2 | R_L | K_F [(mg/g)·(L/mg)] ^{1/n} | 1/n | R^2 |
| Cu^{2+} | 13.81 | 0.6902 | 0.9343 | 0.0282 | 4.1305 | 0.3279 | 0.7773 |
| Ni^{2+} | 20.88 | 0.3236 | 0.9531 | 0.0582 | 4.7086 | 0.6105 | 0.8017 |
| Pb^{2+} | – | – | 0.8328 | – | 9.8434 | 0.3165 | 0.3381 |

The plot of C_e against C_e/q_e and the plot of $\log C_e$ against $\log q_e$ were constructed to determine the parameters of Langmuir–Freundlich equations as displayed in Fig. 6 and Table 5. It was found that the Langmuir equation is more suitable than Freundlich model in the description of the adsorption behavior of Cu^{2+} and Ni^{2+} on the banana-derived ACs with higher values of correlation coefficients (R^2 of 0.93 and 0.95, respectively), while the adsorption of Pb^{2+} appeared less fitted with $R^2 = 0.83$. Moreover, values of R_L were found to be lower than 1, suggesting that the adsorption processes are favorable.

4. Conclusion

The porous activated carbon fabricated from banana peel precursor through KOH activation was found to be an effective adsorbent for removal of Cu^{2+} , Ni^{2+} and Pb^{2+} ions from aqueous solution. The RSM involving CCD was successfully applied to examine the impact of independent variables, including metal ion concentration, pH and AC dosage on the removal of Cu^{2+} , Ni^{2+} , and Pb^{2+} and to determine the optimum adsorption conditions. The quadratic equations developed to model the adsorption of all three metals on the banana peel based activated carbon were proved statistically significant. It is noted that the quadratic models for Ni^{2+}

and Pb^{2+} had the higher goodness of fit than that for Cu^{2+} . Accordingly, the maximum adsorption capacities for Cu^{2+} , Ni^{2+} , and Pb^{2+} were obtained at (14.3 mg/g) < Ni^{2+} (27.4 mg/g) < Pb^{2+} (34.5 mg/g) using the initial concentration of 85 ppm, 90.3 ppm, 74.4 ppm, AC dosage of 2.4 g/L, 1.8 g/L, 0.9 g/L and pH values of 6.5, 6.4, 6.1, respectively. In addition, the adsorption isotherms of Cu^{2+} and Ni^{2+} were found to follow well the Langmuir adsorption principle. The obtained results proved a great potential to apply the low-cost banana peel-derived activated carbon with the well-defined adsorption characteristics for environmental treatment.

Acknowledgments

This research is funded by Foundation for Science and Technology Development, Nguyen Tat Thanh University, Ho Chi Minh City, Vietnam and the KIST Institutional Program (Project no. 2Z04820-16-090).

Reference

- [1] E. Gonzalez-Serrano, T. Cordero, J. Rodriguez-Mirasol, L. Cotoruelo, J.J. Rodriguez, Removal of water pollutants with activated carbons prepared from H_3PO_4 activation of lignin from kraft black liquors, *Water Res.* 38 (2004) 3043–3050.
- [2] G.O. El-Sayed, M. Yehiab, A. Asaad, Assessment of activated carbon prepared from corncob by chemical activation with phosphoric acid, *Water Resour. Ind.* 7–8 (2014) 66–75.
- [3] J. Taya, X. Chena, S. Jeyaseelana, N. Graham, Optimising the preparation of activated carbon from digested sewage sludge and coconut husk, *Chemosphere* 44 (2011) 45–51.
- [4] M. Gratioa, T. Panyathanmaporn, R.-A. Chumnanklang, N. Sirinuntawittaya, A. Dutta, Production of activated carbon from coconut shell: Optimization using response surface methodology, *Bioresour. Technol.* 99 (2008) 4887–4895.
- [5] M. Auta, B.H. Hameed, Preparation of waste tea activated carbon using potassium acetate as an activating agent for adsorption of Acid Blue 25 dye, *Chem. Eng. J.* 171 (2011) 502–509.
- [6] B. Marriyappan, K. Hyun-Chul, S. Wang-Geun, K. Chan, L. Jae-Wook, M. Hee, Preparation of powdered activated carbon from rice husk and its methane adsorption properties, *Korean J. Chem. Eng.* 23 (2006) 663–668.
- [7] K.Y. Foo, L.K. Lee, B.H. Hameed, Preparation of activated carbon from sugarcane bagasse by microwave assisted activation for the remediation of semi-aerobic landfill leachate, *Bioresour. Technol.* 134 (2013) 166–172.
- [8] S. Hashemian, K. Salari, Z. Yazdi, Preparation of activated carbon from agricultural wastes (almond shell and orange peel) for adsorption of 2-pic from aqueous solution, *J. Ind. Eng. Chem.* 20 (2014) 1892–1900.
- [9] M. Yahya, Z. Al-Qodah, C. Ngah, Agricultural bio-waste materials as potential sustainable precursors used for activated carbon production: a review, *Renew. Sustain. Energy Rev.* 46 (2015) 218–235.
- [10] J. Dias, M. Alvim-Ferraz, M. Almeida, J. Rivera-Utrilla, M. Sánchez-Polo, Waste materials for activated carbon preparation and its use in aqueous-phase treatment: a review, *J. Environ. Manag.* 85 (2007) 833–846.
- [11] P. Tchounwou, C. Yedjou, A. Patlolla, D. Sutton, Heavy metal toxicity and the environment, *Mol. Clin. Environ. Toxicol.* 101 (2012) 133–164.
- [12] T. Kurniawan, G. Chan, W.-H. Lo, S. Babel, Physico-chemical treatment techniques for waste water laden with heavy metals, *Chem. Eng. J.* 118 (2006) 83–98.
- [13] S. Flora, M. Mittal, A. Mehta, Heavy metal induced oxidative stress & its possible reversal by chelation therapy, *Indian J. Med. Res.* 128 (2008) 501–523.
- [14] M.A. Barakat, New trends in removing heavy metals from industrial wastewater, *Arab. J. Chem.* 4 (2011) 361–377.
- [15] M. Muhamad, S. Abdullah, A. Mohamad, R. Rahman, A. Kadhum, Application of response surface methodology (RSM) for optimisation of COD, NH_3-N and 2,4-DCP removal from recycled paper wastewater in a pilot-scale granular activated carbon sequencing batch biofilm reactor (GAC-SBBR), *J. Environ. Manag.* 121 (2013) 179–190.
- [16] M. Roosta, M. Ghaedi, R. Sahraei, M. Purkait, Ultrasonic assisted removal of sunset yellow from aqueous solution by zinc hydroxide nanoparticle loaded activated carbon: optimized experimental design, *Mater. Sci. Eng. C* 52 (2015) 82–89.
- [17] B. Hameed, F. Daud, Adsorption studies of basic dye on activated carbon derived from agricultural waste: Hevea brasiliensis seed coat, *Chem. Eng. J.* 139 (2008) 48–55.
- [18] M. Soleimani, T. Kaghazchi, Agricultural waste conversion to activated carbon by chemical activation with phosphoric acid, *Chem. Eng. Technol.* 30 (2007) 649–654.
- [19] J. Wang, S. Kaskel, KOH activation of carbon-based materials for energy storage, *J. Mater. Chem.* 22 (2012) 23710–23725.
- [20] N. Bagheri, J. Abedi, Preparation of high surface area activated carbon from corn by chemical activation using potassium hydroxide, *Chem. Eng. Res. Des.* 87 (2009) 1059–1064.
- [21] T. Otowa, Y. Nojima, T. Miyazaki, Development of KOH activated high surface area carbon and its application to drinking water purification, *Carbon* 35 (1997) 1315–1319.
- [22] L. Xian-Fa, X. Qing, F. Yao, G. Qing-Xiang, Preparation and characterization of activated carbon from Kraft lignin via KOH activation, *Environ. Prog. Sustain. Energy* 33 (2014) 519–526.
- [23] T. Nwabueze, Review article: basic steps in adapting response surface methodology as mathematical modelling for bioprocess optimisation in the food systems, *Int. J. Food Sci. Technol.* 45 (2010) 1768–1776.
- [24] M. Mourabet, A. El Rhilassi, H. El Boujaady, M. Bennani-Ziatni, A. Taitai, Use of response surface methodology for optimization of fluoride adsorption in an aqueous solution by Brushite, *Arab. J. Chem.* (2014) In Press, Corrected Proof–Note to users, doi:10.1016/j.arabj.2013.12.028.
- [25] M. Amini, H. Younesi, Nader Bahramifar, A. Lorestani, F. Ghorbani, A. Daneshia, M. Sharifzadeh, Application of response surface methodology for optimization of lead biosorption in an aqueous solution by *Aspergillus niger*, *J. Hazard. Mater.* 154 (2008) 694–702.
- [26] A. Asfaram, M. Ghaedi, A. Goudarzi, M. Rajabic, Response surface methodology approach for optimization of simultaneous dye and metal ion ultrasound-assisted adsorption onto Mn doped Fe_3O_4 -NPs loaded on AC: kinetic and isothermal studies, *Dalton Trans.* 44 (2015) 14707–14723.
- [27] L. Chen, T. Zhenguang, S. Su, W. Jiang, Characterization of mesoporous activated carbons prepared by pyrolysis of sewage sludge with pyrolusite, *Bioresour. Technol.* 101 (2010) 1097–1101.
- [28] N. Thitiwan, S. Pengpanich, M. Hunsom, Adsorptive desulfurization of dibenzothiophene by sewage sludge-derived activated carbon, *Chem. Eng. J.* 228 (2013) 263–271.
- [29] W. Isahak, M. Hisham, M. Yarmo, Highly porous carbon materials from biomass by chemical and carbonization method: a comparison study, *J. Chem.* 2013 (2013) 1–6, doi:10.1155/2013/620346.
- [30] P. Sugumaran, V. Priya Susan, P. Ravichandran, S. Seshadri, Production and characterization of activated carbon from banana empty fruit bunch and deionix regia fruit pod, *J. Sustain. Energy Environ.* 3 (2012) 125–132.
- [31] I. Gurten, M. Ozmak, E. Yagmur, Z. Aktas, Preparation and characterisation of activated carbon from waste tea using K_2CO_3 , *Biomass Bioenergy* 37 (2012) 73–81.
- [32] X. Jianzhong, H. Lingzhi, Q. Hongqiang, J. Yunhong, X. Jixing, X. Guang, Preparation and characterization of activated carbon from reedy grass leaves by chemical activation with H_3PO_4 , *Appl. Surf. Sci.* 320 (2014) 674–680.
- [33] T. Chandra, M. Mirna, J. Sunarso, Y. Sudaryanto, S. Ismadji, Activated carbon from durian shell: preparation and characterization, *J. Taiwan Inst. Chem. Eng.* 40 (2009) 457–461.
- [34] F. Ghorbani, H. Younesi, G. Seyed, Z. Ali, M. Amini, D. Ali, Application of response surface methodology for optimization of cadmium biosorption in an aqueous solution by *Saccharomyces cerevisiae*, *Chem. Eng. J.* 145 (2008) 267–275.
- [35] K. Kadirvelu, K. Thamaraiselvi, C. Namasivayam, Removal of heavy metals from industrial wastewaters by adsorption onto activated carbon prepared from an agricultural solid waste, *Bioresour. Technol.* 76 (2001) 63–65.
- [36] K. Kadirvelu, C. Faur-Brasquet, P. Cloirec, Removal of Cu (II), Pb (II), and Ni (II) by adsorption onto activated carbon cloths, *Langmuir* 16 (2000) 8404–8409.
- [37] C. Faur-Brasquet, K. Kadirvelu, P. Cloirec, Modeling the adsorption of metal ions (Cu^{2+} , Ni^{2+} , Pb^{2+}) onto ACCs using surface complexation models, *Appl. Surf. Sci.* 196 (2002) 356–365.
- [38] A. Kongsuwan, P. Patnukao, P. Pavasant, Binary component sorption of Cu (II) and Pb (II) with activated carbon from *Eucalyptus camaldulensis* Dehn bark, *J. Ind. Eng. Chem.* 15 (2009) 465–470.
- [39] N. Esfandiari, B. Nasernejad, T. Ebadi, Removal of Mn(II) from groundwater by sugarcane bagasse and activated carbon (a comparative study): application of response surface methodology (RSM), *J. Ind. Eng. Chem.* 20 (2014) 3726–3736.
- [40] Y. Huang, S. Li, J. Chen, X. Zhang, Y. Chena, Adsorption of Pb(II) on mesoporous activated carbons fabricated from water hyacinth using H_3PO_4 activation: Adsorption capacity, kinetic and isotherm studies, *Appl. Surf. Sci.* 293 (2014) 160–168.
- [41] Y. Han, L. Weiwei, J. Zhang, H. Meng, Y. Xua, X. Zhang, Adsorption behavior of Rhodamine B on nanoporous polymers, *RSC Adv.* 5 (2015) 104915–104922.
- [42] T.M. Alslalibi, I. Abustan, MohdA. Ahmad, A.A. Foul, Cadmium removal from aqueous solution using microwave olive stone activated Carbon, *J. Environ. Chem. Eng.* 1 (2013) 589–599.
- [43] Y. Huang, S. Li, H. Lin, J. Chen, Fabrication and characterization of mesoporous activated carbon from Lemna minor using one-step H_3PO_4 activation for Pb(II) removal, *Appl. Surf. Sci.* 317 (2014) 422–431.